Bone morphogenetic protein 9 (BMP9) directly induces Notch effector molecule Hes1 through the SMAD signaling pathway in osteoblasts

Chang-Hwan Seong[1,2], Norika Chiba[2], Joji Kusuyama[2,3,4], Muhammad Subhan Amir[1,2,5], Nahoko Eiraku[6], Sachiko Yamashita[2], Tomokazu Ohnishi[2], Norifumi Nakamura[1] and Tetsuya Matsuguchi[2*]

1 Department of Oral and Maxillofacial Surgery, Kagoshima University Graduate School of Medical and Dental Sciences, Kagoshima, Japan

2 Department of Oral Biochemistry, Kagoshima University Graduate School of Medical and Dental Sciences, Kagoshima, Japan

3 Section on Integrative Physiology and Metabolism, Joslin Diabetes Center, Department of Medicine, Harvard Medical School, One Joslin Place, Boston, MA 02215, USA

4 Frontier Research Institute for Interdisciplinary Sciences, Tohoku University, Sendai, Japan

5 Department of Oral and Maxillofacial Surgery, Faculty of Dentistry, Airlangga University, Surabaya, Indonesia

6 Department of Periodontology, Kagoshima University Graduate School of Medical and Dental Sciences, Kagoshima, Japan

*Address correspondence to: Tetsuya Matsuguchi, Department of Oral Biochemistry, Field of Developmental Medicine, Kagoshima University Graduate School of Medical and Dental Sciences, 8-35-1 Sakuragaoka, Kagoshima 890-8544, Japan, TEL, +81-99-275-6130; Fax, +81-99-275-6138, Email: tmatsugu@dent.kagoshima-u.ac.jp

ABSTRACT

Bone morphogenetic protein (BMP) 9 is one of the most osteogenic BMPs, whereas its mechanism of action has not been fully elucidated. Hes1, a transcriptional regulator with basic helix-loop-helix (bHLH) domain, is a well-known effector of Notch signaling. Here, we have found that BMP9 induces periodic increases of Hes1 mRNA and protein expressions in osteoblasts presumably through an autocrine negative feedback mechanism. BMP9-mediated Hes1 induction was significantly inhibited by an ALK inhibitor and overexpression of Smad7, an inhibitory Smad. Luciferase and chromatin immunoprecipitation assays revealed two Smad binding sites in the 5' upstream region of mouse Hes1 gene are essential for transcriptional activation by BMP9. Thus, our data indicate that BMP9 induces Hes1 expression in osteoblasts via Smad signaling pathway.

Key Words

Bone Morphogenetic Protein 9 (BMP9), Hes1, Notch, Osteogenic differentiation, Bone regeneration

1. Introduction

In recent aging societies, bone loss caused by cancer, trauma, osteoporosis or chronic inflammatory diseases, such as rheumatoid arthritis and periodontal disease, has become a serious social threat. Cytokine-based bone regeneration therapy draws a lot of attention as a promising clinical approach to various chronic bone loss diseases. Bone morphogenetic proteins (BMPs) are a family of osteogenic cytokines belonging to the TGF superfamily and play an important role in stem cell differentiation, skeletal development and bone formation [1-3]. At least 14 different BMPs have been found in humans to date, and a variety of skeletal anomalies occur by disruptions of BMP signaling [4,5].

BMP signal transduction starts with a heterodimeric complex of two transmembrane serine/threonine kinase receptors, BMP type 1 receptors (BMPRI) and BMPR type 2 (BMPRII) [6]. BMPRII are constitutively active and induces the activation of BMPRI through cross-phosphorylation. BMP binding to receptor heterodimers subsequently initiates downstream signaling events: Smad-dependent (canonical) and Smad-independent (non-canonical). In the canonical BMP signaling pathway, receptor-Smads, namely Smad1, 5, and 8, interact directly with activated BMPRI, while common-Smads (Smad4) make complexes with activated receptor-Smads. The heterodimeric Smad complexes translocate to the nucleus as transcription factors, and regulate gene expressions [7]. The BMP signaling pathway is negatively regulated by inhibitory-Smads, namely Smad6 and 7. Smad7 binds to the activated BMPRI, interrupting receptor-Smads from becoming activated. On the other hand, Smad6 can bind to receptor-Smads directly, thus preventing heterodimer complex formation [8,9]. BMPs also induce Smad-independent pathways such as the mitogen-activated protein kinase (ERKs, p38, JNKs) [10]. Moreover, recent studies have illustrated crosstalks between BMP signaling and other signaling pathways [11-17]. However, the detailed activation mechanisms of these signaling pathways have not been well elucidated.

Previous studies have revealed that BMP9 is the most osteogenic cytokine among BMP members promoting osteoblast differentiation of mesenchymal stem cells (MSCs) both in vitro and in vivo [18]. BMP9 (also known as growth differentiation factor 2 or GDF-2) was first identified from fetal mouse liver cDNA libraries and highly expressed in the developing mouse liver [19]. Overexpression of BMP9 in MSCs dramatically increased alkaline phosphatase (ALP) activity and osteocalcin (OCN) expression, markers of the early and late osteogenic differentiation, as well as calcium deposition as represented by Alizarin Red S staining. Furthermore, BMP9 induced ossification earlier than the other BMPs, such as BMP2 and BMP7 in an orthotopic ossification animal model [11,13,18,20]. However, details of BMP9-induced molecular events in osteoblast have not been fully elucidated.

In this study, we investigated Hes1 induction by BMP9 and its molecular mechanisms in osteoblasts. Hes family proteins (Hes1-7) are transcriptional regulators with basic helix-loop-helix (bHLH) domain and is a well-known effector of Notch signaling [21]. Among the Hes genes, Hes1 especially has an indispensable role in regulating neuronal differentiation. Hes1 expression is essential for suppressing neuronal differentiation and maintaining undifferentiated state at the early stage of embryonic development [22-24]. Notch signaling is highly conserved among most animals, and involved in embryonic development and cell fate specification [25-27]. Furthermore, Notch signaling has been reported to function as a significant regulator of bone formation [28]. However, the role of Notch signaling in BMP9-induced osteoblast differentiation remains controversial [14,15].

Here, we demonstrated that Hes1 is a direct target of BMP9 signaling and is upregulated at the immediate early stage of BMP9-induced osteogenic differentiation. This process appears to be independent of Notch signaling and directly mediated by the Smad-dependent pathway. Furthermore, we identified two Smad-binding consensus sites in the 5' upstream region of the mouse Hes1 gene essential for the transcriptional induction by BMP9 in osteoblasts.

2. Materials and Methods

2.1 Animals and Cells

C57BL/6 mice were obtained from CLEA Japan, Inc. (Tokyo, Japan). Primary osteoblasts were isolated from newborn C57BL/6 mouse calvariae as previously described (Matsuguchi 2009 JBMR). The animals were maintained in accordance with protocols approved by the Animal Care and Use Committee at Kagoshima University, Japan. MC3T3-E1 cells were obtained from RIKEN Cell Bank (Tsukuba, Japan), and maintained in Eagle's α-minimal essential medium (αMEM) (Sigma –Aldrich, Inc., St. Louis, MO) containing 10% fetal bovine serum (FBS), 10 mM HEPES (pH 7.2-7.5), 100 units/ml penicillin, and 100 μg/ml streptomycin.

2.2 Antibodies and reagents

Phospho-specific antibodies against Extracellular signal-regulated kinases (ERKs), Smad1/5, as well as the antibody against Hes1 were all purchased from Cell Signaling Technology (Danvers, MA). The antibodies against β-actin and Glyceraldehydes-3-phosphate dehydrogenase (GAPDH) were purchased from Santa Cruz Biotechnology (Santa Cruz, CA) and IMGENEX Corporation (San Diego, CA), respectively. Recombinant mouse BMP9 was obtained from Biolegend, Inc. (San Diego, CA). SP600125, a JNK-specific inhibitor, was from LC Laboratories (Woburn, MA).

LDN193189, a specific ALK (BMP type I receptors) inhibitor, U0126, an ERK-specific inhibitor, SB203080, a p38-specific inhibitor, and LY3039478, a Notch-specific inhibitor, were all purchased from Funakoshi (Tokyo, Japan). Anti-Smad1 and anti-Smad5 for ChIP procedure were purchased from Cell Signaling Technology (Danvers, MA). DMH1, a BMP specific inhibitor, was purchased from Cayman Chemical (USA).

2.3 Western blot analysis

Total cellular lysates were prepared in RIPA cell lysis buffer (150mM NaCl, 5mM EDTA, 1% Deoxycholate, 0.1% SDS, 1% Triton-X) with the addition of 1mM Na_3VO_4 and 1X Proteinase Inhibitor Cocktail (Funakoshi Co., Ltd., Tokyo, Japan). Cell lysates, containing 10 μg protein for each lane, were separated by SDS-PAGE. Immunoblotting was performed as previously described [11]. The antibody concentrations used for immunodetection were 0.2μg/ml for both primary and horseradish peroxidase–conjugated secondary antibodies.

2.4 Real-time PCR analyses

Total RNA was isolated from cells using Isogen II (Nippon Gene Co., Ltd., Tokyo, Japan) and reverse transcription was performed using ReverTra Ace (Toyobo, Tokyo, Japan) according to the manufacturers' instructions. Real-time PCR was conducted using CFX ConnectTM (Bio-Rad, Hercules, CA). Briefly, the cDNA synthesized from 0.05 μg of total RNA was amplified in a volume of 20 μl with 0.11 x SYBR Green I (CAMBREX, Rockland, ME, USA), 0.2 mM/each of dNTPs, 0.5 μM/each of a pair of primers, and 0.5 unit Dream Taq Hot Start DNA polymerase (Thermo Fisher Scientific Inc., Waltham, MA) under the following condition: 95°C for 5 min, followed by 55 PCR cycles at 95°C for 30 s, 60°C for 20 s, and 72°C for 40 s. Fluorescent signals were measured in real time, and then each sample was quantified according to the manufacturer's instructions. The primer sequences used in this study are listed in Table 1. In order to normalize the differences in the amount of total RNA added to each reaction, Ribosomal protein L13a (Rpl13a) was used as the endogenous control. An arbitrary unit was determined by dividing the concentration of each PCR product by the concentration of the Rpl13a PCR product. Each real-time PCR analysis was done in triplicate and repeated at least three times to confirm the consistent results.

2.5 Generation of Hes1 promoter constructs, site-directed mutagenesis, and promoter assay

Mouse Hes1 genomic DNAs containing various lengths of the 5' upstream region of the putative transcriptional initiation site were cloned by PCR from C57BL/6 genomic DNA using a series of primers, sense: CCG CTA GCA ACA TAC AGA GTT CGA GCG G (pGL4.17-500), CCG CTA GCC AGG CGC GCC CTC GCC GGC C (pGL4.17-1000), CCG CTA GCC CAA GCC CGG AGT CCC GGC G (pGL4.17-1500), CCG CTA GCG CTG GGA TCC CGA GCT GCC C (pGL4.17-2000), in combination with the antisense CCA AGC TTC AAG GAG AGA GGT AGA CAG G. All PCR products were ligated into pTAC-1 vector (BioDynamics Laboratory Inc.), digested with NheI and HindⅢ, and the inserts were subcloned into a luciferase reporter vector, pGL4.17 (Promega). To generate site-directed mutagenesis of the putative Smad binding sites of Hes1 gene, mutated DNA fragments constructed by PCR using five primer pairs, GGCTCAGCTTTCGGGCCaCCGCCC (A.sense) and GGAATCCGCGGGGGCGGtGGCC (A.antisense) or CCGGGGACCAGAGGCaGCCC (B.sense) and GAGGGAGCGGGGGCtGCC (B.antisense) or CCGCTCCCTCCCGGCCaGCCG (C.sense) and GGCCGGCGGCGGCtGGCC (C.antisense) or CCCTCCCGGCCGGCCaCCGC (D.sense) and CGGGGGCCGGCGGtGGCC (D.antisense) or GGCCGCAGCCGCGGCaGC (E.sense) and GCCAGGATGTTTTATTGCtGCCGCG (E.antisense) (the putative Hes1 binding sites are underlined, and altered bases are given in lowercase letters), were used to introduce specific mutations into pGL4.17-1500 construct. The resultant mutated plasmids, pGL4.17-(Mut.A, Mut.B, Mut.C, Mut.D, Mut.E, Mut.A&E), and the wild-type control plasmid were transiently transfected into MC3T3-E1 cells by ScreenFect A Plus (Fujifilm Wako Pure Chemicals) according to the manufacturer's instructions. At 48h after the transfection, MC3T3-E1 cells were serum-starved for 16h and stimulated with 50ng/ml BMP9 for 6h. Luciferase activity in the cell lysates was analyzed with ONE-Glo Luciferase Assay System (Promega) according to the manufacturer's instructions.

2.6 Chromatin immunoprecipitation assay

Chromatin immunoprecipitation assay (ChIP) assay was performed as described previously [12]. PCR amplifications were carried out using DreamTaq DNA Polymerase (Thermo Scientific™) under the following condition: 95°C for 5 min, and then 36 PCR cycles at 95°C for 30 s, 60°C for 20 s, and 72°C for 40 s. The Hes1 promoter specific primers were as follows: primer #1 (-1413 to -1204) sense, CTGCCCGGAAGGATTGA and antisense, GCTCGAGCCTGGGAAAAC; and primer #2 (-1200 to -1007), GCAGCTGCTATTTACCTTCTTGG and antisense, AGCACGTGCCAGGATGTTTTA.

The PCR products were analyzed by electrophoresis on a 1.5% agarose gel and quantitative PCR. For each reaction, 1% of crosslink released chromatin was saved and reversed at 55°C for 6 h, followed by proteinase K digestion and DNA extraction. The recovered DNA was used as the input control.

2.7 Tet-on inducible expression system

A Tet-on regulator plasmid, pEF-1a-Tet-on, was prepared by replacing the CMV promoter of a regulator plasmid, pTet-on (Clontech Laboratories, Mountain View, CA, USA), with the human elongation factor 1a (EF-1a) promoter. The pEF-1a-Tet-on was stably transfected into MC3T3-E1 cells by ScreenFect A Plus according to the manufacturer's instructions, followed by selection with 0.5 mg/ml G418. The cDNA of mouse Smad7 was amplified by RT-PCR from the total RNA isolated from MC3T3-E1 cells and cloned into pTRE2-Hyg vector (Clontech Laboratories), which contains the hygromycin-resistance gene. After verification by restriction mapping and sequencing, the constructed inducible expression plasmid, which was termed as pTRE2-Hyg-mSmad7 was stably transfected into the MC3T3-E1 pEF-1a-Tet-on cell line by ScreenFect A Plus. As a negative control cell line, pTRE2-Hyg vector was stably transfected into the MC3T3-E1 pEF1a-Tet-on cell line. After selection with 0.5 mg/ml G418 and 0.3 mg/ml hygromycin B, the isolated resistant clones were tested for the inducible protein expression from the inserted cDNAs with 5 μg/ml doxycycline (DOX). Individual three to five cell lines with good inducible protein expression were analyzed for each construct.

2.8 RNA interference

Small interference RNA (siRNA) was introduced into MC3T3-E1 by using ScreenFect A plus (Fujifilm Wako Pure Chemical Corporation, Osaka, Japan) according to the manufacturer's instruction. The specific siRNAs used in this assay were Smad6: r(GAUUCUACAUUGUCUUACA)dTdT and r(UGUAAGACAAUGUAGAAUC)dTdT, Smad7 (Mission siRNA SASI-Mm02-00290885), and Hes1: r(CCGUAAAGUCCCUAGCCCA)dTdT and r(UGGGCUATGGGACUUUACGG)dTdT obtained from Sigma Aldrich, or non-targeting control siRNA duplexes (Control siRNA-A; Santa Cruz Biotechnology). Total RNA was collected at 48 hours after siRNA introduction for real-time PCR analysis. At 44 hours after siRNA introduction, the cells were placed under serum-free condition for 4 hours followed by 25ng/ml mBMP9, and then whole cell lysates were collected at the indicated time. Target proteins were detected by Western blotting.

3. Results

3.1 Analysis of BMP9-induced Hes1 expression

In the course of analyzing mouse primary osteoblasts for protein expressions induced by osteogenic BMPs, Hes1, a well-established transcriptional modulator of Notch signaling, was found to be rapidly induced by BMP2, 4, and 9. Notably, in a dose response experiment, BMP9 induced Hes1 protein expression more efficiently than BMP2 or 4 (Fig. 1A). Consistently, BMP9 rapidly increased Hes1 mRNA more efficiently than BMP2 or BMP4 in primary osteoblasts (Fig. 1B). To gain further insight into the expression of Hes1 induced by BMP9, MC3T3-E1 cells, a commonly used mouse osteoblast cell line, were stimulated with BMP9 (50 ng/ml) for up to 12 h. When transcriptional activation of Hes1 was analyzed by RT-PCR, periodic increases of Hes1 mRNA expression levels were found after BMP9 stimulation (Fig. 1C). The expression peak was observed after 1 hour and exhibited a 2-hour cycle oscillation until 6 hours after BMP9 stimulation. In western blotting analysis, Hes1 protein displayed a similar periodic pattern of production induced by BMP9 (Fig. 1D).

To further analyze the mechanism of oscillatory expression of Hes1, MC3T3-E1 cells were stimulated with BMP9 (10 ng/ml) with or without MG132, a proteasome inhibitor. The results showed that the protein level of total Smad5 was not affected by MG132, and MG132 alone did not induce the phosphorylation of Smad1/5 (Fig.1E). Notably, MG132 suppressed the degradation of Hes1 protein induced by BMP9 resulting in the abrogation of the periodic expression pattern of Hes1 mRNA (Fig.1E, 1F). Therefore, it seems reasonable to conclude that proteasome-dependent Hes1 protein degradation is essential for the periodic expression pattern of Hes1 mRNA in BMP9-stimulated osteoblasts.

3.2 Identification of responsible pathways for BMP9-induced Hes1 expression

In order to identify the intracellular signal transduction mechanism of BMP9-induced Hes1 expression, we examined the effects of specific chemical inhibitors. We first found that pretreatment of serum-starved MC3T3-E1 cells with LDN193189, an inhibitor of BMP type 1 receptor, ALK1, ALK2, ALK3, and ALK6, significantly suppressed BMP9-induced Hes1 expression in osteoblasts (Fig. 2A). Since LDN193189 potently inhibits the kinase activity of BMP type 1 receptors, which is essential for Smad activation [29], these results indicate the possible involvement of Smad1/5-mediated signaling pathway in BMP9-induced Hes1 expression. On the other hand, pretreatment with LY3039478 (a specific γ-secretase complex inhibitor), U0126 (a specific ERK1, 2 inhibitor), SB203580 (a specific p38 inhibitor) or

SP600125 (a specific JNK inhibitor) showed no effect on BMP9-induced Hes1 expression (Fig. 2B, 2C, 2D).

For more specific inhibition of Smad signaling pathways, we established MC3T3-E1 cell lines with inducible expression of an inhibitory Smad, Smad7, using the Tet-On system (Fig. 2E, 2F). It was found that the induced expressions of Smad7 significantly suppressed the BMP9-mediated protein expression of Hes1 as well as Smad1/5 phosphorylation (Fig. 2E). Notably, Smad7 induction also suppressed the BMP9-mediated mRNA expression of Hes1 (Fig. 2F). We also introduced small interference RNA (siRNA) designed for either Smad7 or Smad6 into MC3T3-E1 cells. The suppressive effects of Smad6 or Smad7 siRNA transfections were confirmed by decreased mRNA expression levels of the target genes (Fig. 2G). Notably, knockdown of either Smad6 or Smad7 significantly enhanced protein expression of Hes1 compared with Control (Fig. 2H).

Two inhibitory Smads, namely Smad6 and 7 can interrupt not only the BMP signaling pathway but also the phosphorylation of Smad2/3 which is related with TGF-² signaling [30,31]. To confirm the specific requirement of Smad1/5/8 for BMP9-induced Hes1 expression, DMH1 is used as a Smad1/5/8-specific inhibitors [32-34]. Previous studies have revealed that DMH1 selectively inhibited the activation of Smad1/5/8 induced by BMP treatment, but not the p38/MAP kinase signaling [34,35]. Furthermore, DMH1 had no effect on Activin A-induced Smad2 phosphorylation in HEK293 cells [34]. We found that pretreatment of MC3T3-E1 cells with DMH1 significantly suppressed both BMP9-induced Hes1 expression and the phosphorylation of Smad1/5 in osteoblasts. (Fig. 2I).

Taken together, these results strongly indicate that BMP9 induces the expression of Hes1 via the Smad1/5 activation pathway, but not Notch or MAP kinase signaling pathways, in osteoblasts.

3.3 Identification of BMP9-responsive region in Hes1 promoter

To explore the possibility that activated Smad1/5 protein may bind to the transcriptional regulatory region of the Hes1 gene, we carried out luciferase promoter assays. Luciferase reporter plasmids containing various lengths of the Hes1 gene 5' upstream region were constructed and transfected into MC3T3-E1 cells (Fig. 3A). By measuring luciferase activities after BMP9 stimulation, we found that BMP9-induced promoter activity was not observed for constructs shorter than 1500 bp upstream of the transcription start site of the Hes1 gene (Fig. 3B), indicating that the BMP9-responsive regulatory region exists in the -1500 ~ -1000 bp region.

3.4 Identification of the Smad binding sites in the Hes1 gene promoter region

In order to identify a possible Smad1/5-mediated mechanism of Hes1 transcriptional activation, we searched the -1500 ~ -1000 bp upstream region of the mouse Hes1 gene for putative SMAD binding sites. Previous reports revealed that SMAD has been shown to bind to GC-rich sequences (5'-G(G/C)CG(G/C)C-3') as Smad-binding elements (SBEs) in the enhancer regions of the target promoters and activate transcription [36-40]. We found five potential SMAD binding sites located at -1346/1341, -1160/1155, -1139/1134, -1135/1130 and -1036/1031 bp upstream sites (Fig. 4A). To identify the functionally essential sites, these putative SMAD binding elements were independently mutated by site-directed mutagenesis in the -1500 bp construct (Fig. 4B). The resultant mutated plasmids, pGL4.17-Mut.A, Mut.B, Mut.C, Mut.D, Mut.E, and Mut.A&E, as well as the wild-type control construct were transiently transfected into MC3T3-E1 cells. At 48h after the transfection, MC3T3-E1 cells were serum-starved for 16h and stimulated with 50ng/ml BMP9 for 6h, and the luciferase reporter activities were measured. The results indicate that the BMP9-stimulated reporter activity was significantly diminished when either region A or E was mutated (Fig. 4C). The promoter activity was totally abrogated by the double mutation (Mut.A&E). Therefore, Hes1 transcriptional activity is presumably regulated by these two Smad binding sites in BMP9-stimulated osteoblasts.

In order to examine the actual Smad1/5 protein binding of these sites, we performed ChIP assay using an antibody specific to Smad1/5. The presence of the Smad binding sequences in the immunoprecipitated chromatin was analyzed by PCR amplification of the two Hes1 gene 5' upstream regions (-1413/1204 and -1200/1007) (Fig. 4B). The ChIP assay results showed Smad1/5 binding to both -1346/1341 and -1036/1031 of the Hes1 5' upstream region after BMP9 stimulation (Fig. 4D). Taken together, these results have suggested that the two Smad binding sites in 5' upstream region (-1346/1341 and -1036/1031) are functionally essential for the activation of Hes1 promoter in early response of BMP9 stimulation.

3.5 Functional roles of Hes1 on BMP9-induced osteoblast differentiation.

In order to elucidate the functional role of Hes1 on BMP9-induced osteoblast differentiation, we performed siRNA-mediated gene knockdown experiments. Introduction of Hes1-specific siRNAs into MC3T3-E1 cells significantly decreased mRNA expression of Hes1 induced by BMP9. Notably, knockdown of Hes1 significantly enhanced BMP9-induced osteocalcin (Ocn) mRNA levels (Fig. 5A).

4. Discussion

Previous studies have reported BMP9 as one of the most potent osteogenic BMPs [13,18-20], whereas the molecular mechanisms underlying BMP9-induced osteogenesis have not been fully elucidated. To gain insights into the molecular basis of BMP9-mediated osteogenesis, we searched for proteins whose expression is significantly elevated early in osteoblasts after BMP9 stimulation. By using mouse primary osteoblasts, we found that BMP9 rapidly upregulated the protein expression of Hes1 more efficiently than two other osteogenic BMPs, BMP2 and 4 (Fig. 1A, 1B). As Hes1 is a well-known Notch signaling mediator, this finding suggests the possible crosstalk of Notch and BMP9 signaling pathways.

Notch signaling system is highly conserved among most animals and plays essential roles in multiple cellular differentiation processes [41,42]. Although Notch signaling is known to be a key mediator of bone formation [28], its exact role in BMP-induced osteogenic differentiation is still controversial. For example, several previous reports have indicated that activation of Notch signaling promotes BMP-induced ALP activity and calcified nodule formation in vitro [43,44]. On the other hand, other researchers have demonstrated that Notch signaling negatively regulates BMP-induced osteogenic differentiation of mesenchymal progenitor cells [14,16,45,46]. Although the underlining mechanisms of these differences are not clearly understood, these previous findings may indicate a versatile and complicated involvement of Notch signaling in bone metabolism.

Our present results have revealed that BMP9 induces the expression of Hes1, an important effector molecule of Notch signaling, in osteoblasts in a direct manner independent of the expression of Notch and its ligands. Hes family genes (Hes1-7) encode basic helix-loop-helix (bHLH)-type transcriptional repressors that contain a bHLH domain in the N-terminal region for DNA binding and dimerization, and a WRPW motif for co-repressor recruitment [47]. Hes homodimers as well as heterodimers containing other bHLH transcription repressors bind N-box consensus sequences for active repression of target genes [47]. Several Hes members (Hes1, Hes5, and Hes7) were reported to be significantly induced by Notch signaling and are considered as pivotal Notch effectors. Hes1 is the most well-established and well-studied Notch effector among Hes members, and previous reports have shown that Hes1 modulates numerous biological events by repressing the expression of target genes that regulate cell genesis and differentiation. For example, Hes1 is all known to suppress neuronal differentiation and maintains undifferentiated state at the early stage of embryonic development [47]. However, whether Hes1 also plays a pivotal role in BMP-induced osteoblast differentiation remains

mostly enigmatic.

BMP9 stimulation induced a periodic expression pattern of Hes1 mRNA in MC3T3-E1 cells. Hes1 mRNA expression initially peaks at 1 hour and exhibited a 2-hour cycle oscillation until 6 hours after BMP9 stimulation (Fig. 1C). A part of our result is consistent with a previous report which showed the oscillating expression of Hes1 with an average of 2-3 hour cycles in neural progenitors [47-49]. The Hes1 gene promoter contains multiple N-box consensus sequences so that Hes1 gene expression is known to be under the control of autocrine negative-feedback mechanism in neural cells [47]. As inhibition of Hes1 protein degradation by a proteasomal inhibitor suppressed the periodic expression pattern of Hes1 mRNA (Fig. 1F), it is presumed that BMP9-induced Hes1 expression is oscillated by a combination of two mechanisms: the transcriptional repression of Hes1 mRNA by negative autofeedback and the fast degradation of Hes1 protein by proteasome. Similar periodic expression patterns of Hes1 expression were reported in neural cells [47]. Notably, Notch signaling oscillations have been reported to be essential for the regulation of both stemness and differentiation of neural progenitor cells [48]. It may be reasonable to hypothesize that BMP9 regulates the initiation process of osteoblast differentiation through the periodic expression of Hes1 protein. This hypothesis is currently under investigation (data not shown).

Our present study demonstrates that BMP9 induces the expression of Hes1 via Smad pathway but not Notch and MAP kinases in osteoblasts (Fig. 2). Although Hes1 expression is mainly regulated by evolutionarily conserved Notch signaling pathway, LY3039478 (a specific γ-secretase complex inhibitor) did not affect Hes1 production induced by BMP9 in MC3T3-E1 cell (Fig. 2B, 2C), suggesting that Notch signaling is not involved in the process. Several previous studies have revealed Notch-independent Hes1 expression in neuroblastoma cells and retinal progenitors [17,50,51]. Although pretreatment with specific inhibitors of MAP kinases had no effect, pretreatment with LDN193189, a specific ALK inhibitor, significantly inhibited BMP9-induced Hes1 expression (Fig. 2A, 2D). Furthermore, overexpression of Smad7, an inhibitory Smad, diminished the periodic expression of Hes1 mRNA (Fig. 2F). More notably, pretreatment with DMH1, a BMP-specific inhibitor, dramatically inhibited both BMP9-induced Hes1 expression and the phosphorylation of Smad1/5. These results strongly indicate that BMP9 directly induces Hes1 expression via Smad activation.

By performing sequential deletion analysis of mouse Hes1 gene regulatory region, we found that the BMP9-responsive regulatory region exists between -1500 and -1000 bp upstream of the transcription initiation site (Fig. 3B). Among the five potential Smad binding sites in the region, BMP9-responsive transcriptional activity was diminished when either -

1346/1341 or -1036/1031 bp site was mutated (Fig. 4C). In addition, the promoter activity was abrogated by the double mutation. Consistently, ChIP assay with anti-Smad1/5 antibody revealed Smad protein binding to both of these two sites in a manner dependent on BMP9 stimulation (Fig. 4D). Additionally, we have confirmed that the two Smad binding sites in the 5' upstream region of the mouse Hes1 gene are well conserved almost at the same position in both rat and human Hes1 genes (data not shown). Taken together, our study indicates that BMP9 directly induces Hes1 expression via two Smad binding elements in the 5' regulatory region of the Hes1 gene.

Previously, Id proteins was determined as typical BMP responsive genes in various types of cells [52,53]. BMP Responsive Element (BRE), which is a GC rich sequence to which BMP responsive Smads bind [54,55], is found in Id1 [56], Id2 [57] and Id3 [58] gene regulatory regions. More specifically, the 5' upstream regulatory region of the mouse Id1 gene [59] contains GGCGCC sequence which matches the Smad-binding element (SBE) consensus sequence (5'-G(G/C)CG(G/C)C-3'). Furthermore, this GGCGCC sequence is well conserved in the 5' upstream region of the human Id1 gene (data not shown). Interestingly, previous reports revealed that Id proteins can relieve the repressive action of Hes1 by directly interacting with Hes1 [60,61]. Therefore, it seems reasonable to presume that Smad1/5 activation by BMP9 induces not only Hes1 but also other BMP responsive proteins, which then influence Hes1 expression.

On the other hand, another paper reported that BMP4-mediated mRNA expressions of Id1 and Id3 were significantly inhibited by a p38 MAPK inhibitor, but not ERK or JNK inhibitors in lymphocytes [62]. It means that although some Id are BMP-responsive, they are affected by other pathways besides the Smad pathway. These results collectively suggest that our study provides novel findings that Hes1 gene has a different mechanism of action from the other BMP-responsive genes.

Furthermore, a previous study has also reported that BMP9 stimulation enhances the expression of Hey1, another effector molecule of Notch signaling, in a manner independent of Notch and its ligands [63]. Our previous study showed that BMP9-induced Hey1 mRNA expression was significantly suppressed by p38 inhibitor, and promoted by JNK inhibitor in osteoblasts [12]. On the other hand, our current study newly demonstrates that BMP9 induces the expression of Hes1 through Smad pathway but not Notch and MAP kinases in osteoblasts (Fig. 2). This finding also provides new insights into revealing exact role of Notch signaling in BMP-induced osteogenic differentiation.

A previous study revealed four N box sequences in the mouse Hes1 gene promoter (at nucleotides -165, -132, -58, and +16) by transcriptional analysis of the Hes1 promoter region between nucleotides -2000 and +46, and found that they are essential for the negative autoregulation of Hes1 transcription [21]. Another paper reported that Hes1 is a

transcriptional target of TGF-β1 in smooth muscle cells and scanning of the Hes1 promoter elucidated Smad consensus binding elements within its proximal promoter (-199 to +46) which are activated by Smad2 but not Smad3 [64]. On the other hand, our current study revealed that two Smad consensus binding sites between -1500 and -1000 bp of the Hes1 gene promoter are essential for the transcriptional induction by BMP9, whereas the proximal promoter region (-500 to 0 bp) is not responsive. Furthermore, ChIP assay demonstrated that Smad1/5 activate the Hes1 promoter by BMP9 in osteoblasts. Thus, it reasonable to suggest that BMP9, which mainly activates Smad1/5, induces Hes1 expression in a different manner from TGF-β.

Ocn is a representative marker of late osteoblast differentiation and a regulator of bone mineralization [65]. A previous study reported that Notch-responsive Hes1 protein represses transcription of Ocn gene through binding its gene promoter [66]. This data corresponds with our novel findings that knockdown of Hes1 markedly increased BMP9-induced osteocalcin (Ocn) mRNA levels (Fig. 5A). Other reports revealed that Hes1 is an intracellular determinant of bone mass and structure in vitro and in vivo [67]. Therefore, it may be reasonable to hypothesize that BMP9 regulates the process of osteoblast differentiation through the expression of Hes1. The role of Hes1 in osteogenesis seems rather complicated depending on the osteogenic differentiation stage, and will be clarified in our further studies.

In summary, our finding that BMP9 strongly induces Hes1 expression may provide clues to elucidate the reason why BMP9 has a powerful osteogenic differentiation potential than other BMPs. Interestingly, BMP9-induced Hes1 expression in osteoblasts is oscillated presumably due to an autocrine transcriptional negative feedback mechanism accompanied by rapid proteasomal degradation of Hes1 protein. This finding may indicate that spatiotemporal expression of Hes1 at the cellular level obviously control the adequate orchestration of cell differentiation in BMP9-induced osteoblast differentiation. Altogether, our study provides novel insights into the more effective bone regeneration therapy with BMP9 by further identifying the signaling pathway of BMP9 and the functional role of Hes1.

Acknowledgment

We thank Ms. Yoko Amita and Ms. Tomomi Fujii for the secretarial assistance. This work was supported by grants from the Ministry of Education, Culture, Sports, Science.

Conflicts of interest

The authors declare that they have no conflicts of interest with the contents of this article.

Author contributions

CHS and TM designed research; NC, JK, MSA, NE, SY, TO, NN and TM provided technical assistance for analysis data; CHS, NC and TM performed research; CHS, NC and TM wrote the paper.

References

[1] Urist, M.R. (1965). Bone: formation by autoinduction. Science 150, 893-9.

[2] Beederman, M. et al. (2013). BMP signaling in mesenchymal stem cell differentiation and bone formation. J Biomed Sci Eng 6, 32-52.

[3] Brazil, D.P., Church, R.H., Surae, S., Godson, C. and Martin, F. (2015). BMP signalling: agony and antagony in the family. Trends Cell Biol 25, 249-64.

[4] Zhang, J. and Li, L. (2005). BMP signaling and stem cell regulation. Dev Biol 284, 1-11.

[5] Wang, R.N. et al. (2014). Bone Morphogenetic Protein (BMP) signaling in development and human diseases. Genes Dis 1, 87-105.

[6] Poniatowski, L.A., Wojdasiewicz, P., Gasik, R. and Szukiewicz, D. (2015). Transforming growth factor Beta family: insight into the role of growth factors in regulation of fracture healing biology and potential clinical applications. Mediators Inflamm 2015, 137823.

[7] Massague, J., Seoane, J. and Wotton, D. (2005). Smad transcription factors. Genes Dev 19, 2783-810.

[8] Tsunobuchi, H., Ishisaki, A. and Imamura, T. (2004). Expressions of inhibitory Smads, Smad6 and Smad7, are differentially regulated by TPA in human lung fibroblast cells. Biochem Biophys Res Commun 316, 712-9.

[9] Zhao, J., Shi, W., Chen, H. and Warburton, D. (2000). Smad7 and Smad6 differentially modulate transforming growth factor beta -induced inhibition of embryonic lung morphogenesis. J Biol Chem 275, 23992-7.

[10] Bragdon, B., Moseychuk, O., Saldanha, S., King, D., Julian, J. and Nohe, A. (2011). Bone morphogenetic proteins: a critical review. Cell Signal 23, 609-20.

[11] Eiraku, N. et al. (2019). BMP9 directly induces rapid GSK3-beta phosphorylation in a Wnt-independent manner through class I PI3K-Akt axis in osteoblasts. FASEB J 33, 12124-12134.

[12] Kusuyama, J. et al. (2019). BMP9 prevents induction of osteopontin in JNK-inactivated osteoblasts via Hey1-Id4 interaction. Int J Biochem Cell Biol 116, 105614.

[13] Wu, N., Zhao, Y., Yin, Y., Zhang, Y. and Luo, J. (2010). Identification and analysis of type II TGF-beta receptors in BMP-9-induced osteogenic differentiation of C3H10T1/2 mesenchymal stem cells. Acta Biochim Biophys Sin (Shanghai) 42, 699-708.

[14] Wang, N., Liu, W., Tan, T., Dong, C.Q., Lin, D.Y., Zhao, J., Yu, C. and Luo, X.J. (2017). Notch signaling negatively regulates BMP9-induced osteogenic differentiation of mesenchymal progenitor cells by inhibiting JunB expression. Oncotarget 8, 109661-109674.

[15] Cui, J. et al. (2019). BMP9-induced osteoblastic differentiation requires functional Notch signaling in mesenchymal stem cells. Lab Invest 99, 58-71.

[16] Zamurovic, N., Cappellen, D., Rohner, D. and Susa, M. (2004). Coordinated activation of notch, Wnt, and

transforming growth factor-beta signaling pathways in bone morphogenic protein 2-induced osteogenesis. Notch target gene Hey1 inhibits mineralization and Runx2 transcriptional activity. J Biol Chem 279, 37704-15.

[17] Stockhausen, M.T., Sjolund, J. and Axelson, H. (2005). Regulation of the Notch target gene Hes-1 by TGFalpha induced Ras/MAPK signaling in human neuroblastoma cells. Exp Cell Res 310, 218-28.

[18] Kang, Q. et al. (2004). Characterization of the distinct orthotopic bone-forming activity of 14 BMPs using recombinant adenovirus-mediated gene delivery. Gene Ther 11, 1312-20.

[19] Song, J.J., Celeste, A.J., Kong, F.M., Jirtle, R.L., Rosen, V. and Thies, R.S. (1995). Bone morphogenetic protein-9 binds to liver cells and stimulates proliferation. Endocrinology 136, 4293-7.

[20] Luu, H.H. et al. (2007). Distinct roles of bone morphogenetic proteins in osteogenic differentiation of mesenchymal stem cells. J Orthop Res 25, 665-77.

[21] Takebayashi, K., Sasai, Y., Sakai, Y., Watanabe, T., Nakanishi, S. and Kageyama, R. (1994). Structure, chromosomal locus, and promoter analysis of the gene encoding the mouse helix-loop-helix factor HES-1. Negative autoregulation through the multiple N box elements. J Biol Chem 269, 5150-6.

[22] Ishibashi, M., Ang, S.L., Shiota, K., Nakanishi, S., Kageyama, R. and Guillemot, F. (1995). Targeted disruption of mammalian hairy and Enhancer of split homolog-1 (HES-1) leads to up-regulation of neural helix-loop-helix factors, premature neurogenesis, and severe neural tube defects. Genes Dev 9, 3136-48.

[23] Nakamura, Y., Sakakibara, S., Miyata, T., Ogawa, M., Shimazaki, T., Weiss, S., Kageyama, R. and Okano, H. (2000). The bHLH gene hes1 as a repressor of the neuronal commitment of CNS stem cells. J Neurosci 20, 283-93.

[24] Ohtsuka, T., Sakamoto, M., Guillemot, F. and Kageyama, R. (2001). Roles of the basic helix-loop-helix genes Hes1 and Hes5 in expansion of neural stem cells of the developing brain. J Biol Chem 276, 30467-74.

[25] Nye, J.S. and Kopan, R. (1995). Developmental signaling. Vertebrate ligands for Notch. Curr Biol 5, 966-9.

[26] Artavanis-Tsakonas, S., Matsuno, K. and Fortini, M.E. (1995). Notch signaling. Science 268, 225-32.

[27] Simpson, P. (1995). Developmental genetics. The Notch connection. Nature 375, 736-7.

[28] Zanotti, S. and Canalis, E. (2016). Notch Signaling and the Skeleton. Endocr Rev 37, 223-53.

[29] Yu, P.B. et al. (2008). BMP type I receptor inhibition reduces heterotopic [corrected] ossification. Nat Med 14, 1363-9.

[30] Hayashi, H. et al. (1997). The MAD-related protein Smad7 associates with the TGFbeta receptor and functions as an antagonist of TGFbeta signaling. Cell 89, 1165-73.

[31] Imamura, T., Takase, M., Nishihara, A., Oeda, E., Hanai, J., Kawabata, M. and Miyazono, K. (1997). Smad6 inhibits signalling by the TGF-beta superfamily. Nature 389, 622-6.

[32] Cross, E.E., Thomason, R.T., Martinez, M., Hopkins, C.R., Hong, C.C. and Bader, D.M. (2011). Application of small organic molecules reveals cooperative TGFbeta and BMP regulation of mesothelial cell behaviors. ACS Chem Biol 6, 952-61.

[33] Hao, J. et al. (2014). DMH1, a small molecule inhibitor of BMP type i receptors, suppresses growth and invasion of lung cancer. PLoS One 9, e90748.

[34] Hao, J. et al. (2010). In vivo structure-activity relationship study of dorsomorphin analogues identifies selective VEGF and BMP inhibitors. ACS Chem Biol 5, 245-53.

[35] Huang, R.L., Yuan, Y., Tu, J., Zou, G.M. and Li, Q. (2014). Opposing TNF-alpha/IL-1beta- and BMP-2-activated MAPK signaling pathways converge on Runx2 to regulate BMP-2-induced osteoblastic

differentiation. Cell Death Dis 5, e1187.

[36] Miyazono, K., Kamiya, Y. and Morikawa, M. (2010). Bone morphogenetic protein receptors and signal transduction. J Biochem 147, 35-51.

[37] Ishida, W. et al. (2000). Smad6 is a Smad1/5-induced smad inhibitor. Characterization of bone morphogenetic protein-responsive element in the mouse Smad6 promoter. J Biol Chem 275, 6075-9.

[38] Morikawa, M., Koinuma, D., Tsutsumi, S., Vasilaki, E., Kanki, Y., Heldin, C.H., Aburatani, H. and Miyazono, K. (2011). ChIP-seq reveals cell type-specific binding patterns of BMP-specific Smads and a novel binding motif. Nucleic Acids Res 39, 8712-27.

[39] Sakaki-Yumoto, M., Katsuno, Y. and Derynck, R. (2013). TGF-beta family signaling in stem cells. Biochim Biophys Acta 1830, 2280-96.

[40] Kanamori, Y., Murakami, M., Matsui, T. and Funaba, M. (2017). Identification of novel bone morphogenetic protein- responsive elements in a hepcidin promoter. FEBS Lett 591, 3895-3905.

[41] Canalis, E. (2008). Notch signaling in osteoblasts. Sci Signal 1, pe17.

[42] Zanotti, S., Smerdel-Ramoya, A., Stadmeyer, L., Durant, D., Radtke, F. and Canalis, E. (2008). Notch inhibits osteoblast differentiation and causes osteopenia. Endocrinology 149, 3890-9.

[43] Tezuka, K., Yasuda, M., Watanabe, N., Morimura, N., Kuroda, K., Miyatani, S. and Hozumi, N. (2002). Stimulation of osteoblastic cell differentiation by Notch. J Bone Miner Res 17, 231-9.

[44] Nobta, M., Tsukazaki, T., Shibata, Y., Xin, C., Moriishi, T., Sakano, S., Shindo, H. and Yamaguchi, A. (2005). Critical regulation of bone morphogenetic protein-induced osteoblastic differentiation by Delta1/Jagged1-activated Notch1 signaling. J Biol Chem 280, 15842-8.

[45] Hilton, M.J. et al. (2008). Notch signaling maintains bone marrow mesenchymal progenitors by suppressing osteoblast differentiation. Nat Med 14, 306-14.

[46] Engin, F. et al. (2008). Dimorphic effects of Notch signaling in bone homeostasis. Nat Med 14, 299-305.

[47] Kageyama, R., Ohtsuka, T. and Kobayashi, T. (2007). The Hes gene family: repressors and oscillators that orchestrate embryogenesis. Development 134, 1243-51.

[48] Shimojo, H., Ohtsuka, T. and Kageyama, R. (2008). Oscillations in notch signaling regulate maintenance of neural progenitors. Neuron 58, 52-64.

[49] Shimojo, H., Isomura, A., Ohtsuka, T., Kori, H., Miyachi, H. and Kageyama, R. (2016). Oscillatory control of Delta-like1 in cell interactions regulates dynamic gene expression and tissue morphogenesis. Genes Dev 30, 102-16.

[50] Hashimoto, T., Zhang, X.M., Chen, B.Y. and Yang, X.J. (2006). VEGF activates divergent intracellular signaling components to regulate retinal progenitor cell proliferation and neuronal differentiation. Development 133, 2201-10.

[51] Zhang, S.S., Liu, M.G., Kano, A., Zhang, C., Fu, X.Y. and Barnstable, C.J. (2005). STAT3 activation in response to growth factors or cytokines participates in retina precursor proliferation. Exp Eye Res 81, 103-15.

[52] Hollnagel, A., Oehlmann, V., Heymer, J., Ruther, U. and Nordheim, A. (1999). Id genes are direct targets of bone morphogenetic protein induction in embryonic stem cells. J Biol Chem 274, 19838-45.

[53] Clement, J.H., Marr, N., Meissner, A., Schwalbe, M., Sebald, W., Kliche, K.O., Hoffken, K. and Wolfl, S. (2000). Bone morphogenetic protein 2 (BMP-2) induces sequential changes of Id gene expression in the breast cancer cell line MCF-7. J Cancer Res Clin Oncol 126, 271-9.

[54] Lopez-Rovira, T., Chalaux, E., Massague, J., Rosa, J.L. and Ventura, F. (2002). Direct binding of Smad1

and Smad4 to two distinct motifs mediates bone morphogenetic protein-specific transcriptional activation of Id1 gene. J Biol Chem 277, 3176-85.

[55] Brugger, S.M. et al. (2004). A phylogenetically conserved cis-regulatory module in the Msx2 promoter is sufficient for BMP-dependent transcription in murine and Drosophila embryos. Development 131, 5153-65.

[56] Korchynskyi, O. and ten Dijke, P. (2002). Identification and functional characterization of distinct critically important bone morphogenetic protein-specific response elements in the Id1 promoter. J Biol Chem 277, 4883-91.

[57] Kurooka, H., Nakahiro, T., Mori, K., Sano, K. and Yokota, Y. (2012). BMP signaling is responsible for serum-induced Id2 expression. Biochem Biophys Res Commun 420, 281-7.

[58] Shepherd, T.G., Theriault, B.L. and Nachtigal, M.W. (2008). Autocrine BMP4 signalling regulates ID3 proto-oncogene expression in human ovarian cancer cells. Gene 414, 95-105.

[59] Katagiri, T., Imada, M., Yanai, T., Suda, T., Takahashi, N. and Kamijo, R. (2002). Identification of a BMP-responsive element in Id1, the gene for inhibition of myogenesis. Genes Cells 7, 949-60.

[60] Jogi, A., Persson, P., Grynfeld, A., Pahlman, S. and Axelson, H. (2002). Modulation of basic helix-loop-helix transcription complex formation by Id proteins during neuronal differentiation. J Biol Chem 277, 9118-26.

[61] Bai, G. et al. (2007). Id sustains Hes1 expression to inhibit precocious neurogenesis by releasing negative autoregulation of Hes1. Dev Cell 13, 283-97.

[62] Fiori, J.L., Billings, P.C., de la Pena, L.S., Kaplan, F.S. and Shore, E.M. (2006). Dysregulation of the BMP-p38 MAPK signaling pathway in cells from patients with fibrodysplasia ossificans progressiva (FOP). J Bone Miner Res 21, 902-9.

[63] Sharff, K.A. et al. (2009). Hey1 basic helix-loop-helix protein plays an important role in mediating BMP9-induced osteogenic differentiation of mesenchymal progenitor cells. J Biol Chem 284, 649-59.

[64] Kennard, S., Liu, H. and Lilly, B. (2008). Transforming growth factor-beta (TGF- 1) down-regulates Notch3 in fibroblasts to promote smooth muscle gene expression. J Biol Chem 283, 1324-33.

[65] Neve, A., Corrado, A. and Cantatore, F.P. (2013). Osteocalcin: skeletal and extra-skeletal effects. J Cell Physiol 228, 1149-53.

[66] Zhang, Y., Lian, J.B., Stein, J.L., van Wijnen, A.J. and Stein, G.S. (2009). The Notch-responsive transcription factor Hes-1 attenuates osteocalcin promoter activity in osteoblastic cells. J Cell Biochem 108, 651-9.

[67] Zanotti, S., Smerdel-Ramoya, A. and Canalis, E. (2011). HES1 (hairy and enhancer of split 1) is a determinant of bone mass. J Biol Chem 286, 2648-57.

TABLE 1

Primer sequences used in this study

Gene		Primer sequence [5'- 3']	Product size
Rpl13a	Forward	GCTTACCTGGGGCGTCTG	149 bp
	Reverse	ACATTCTTTTCTGCCTGTTTCC	
Hes1	Forward	GATAGCTCCCGGCATTCCAA	157 bp
	Reverse	CGTTCATGCACTCGCTGAAG	
Smad6	Forward	CATCACTGCTCCGGGTGAAT	128 bp
	Reverse	GGTCGTACACCGCATAGAGG	
Smad7	Forward	TTTCTCAAACCAACTGCAGGC	186 bp
	Reverse	GACACAGTAGAGCCTCCCCA	
Osteocalcin	Forward	CTCACAGATGCCAAGCCCA	98 bp
	Reverse	CCAAGGTAGCGCCGGAGTCT	

Figure 1.

Hes1, a Notch effector molecule, is immediately induced by BMP9. (A) Dose response of Hes1 protein expression in BMP-stimulated osteoblasts. Calvaria-derived mouse primary osteoblasts were stimulated with indicated concentrations of BMP9, BMP2, or BMP4 for 1h. Cell lysates (10μg total protein for each lane) were analyzed with the indicated antibodies by western blotting. Photographical analyses of Hes1/b-Actin expression ratios are shown in the right graph. (B) After serum-starvation for 4h, mouse primary osteoblasts were stimulated with BMP9, BMP2, or BMP4 (10 ng/ml) for 1 hour. Total RNA was isolated and quantitative real-time PCR analyses were performed in triplicate using the specific primers for Hes1. Rpl13a was used as the endogenous control for normalization. (C) After serum-starvation for 4h, MC3T3-E1 cells were stimulated with BMP9 (50 ng/ml) for the indicated hours. Total RNA was isolated and reverse-transcribed. Quantitative real-time PCR analyses were performed in triplicate using the specific primers for Hes1. Rpl13a was used as the endogenous control for normalization. (D) After serum-starvation for 4h, MC3T3-E1 cells were stimulated with BMP9 (50 ng/ml) for the indicated hours. Cell lysates were analyzed with the indicated antibodies by Western blotting. (E) MC3T3-E1 cells were stimulated with BMP9 (10 ng/ml) with or without 10μg/ml of MG132 (Proteasome inhibitor) for the indicated time. Cell lysates were analyzed with the indicated antibodies by western blotting. (F) MC3T3-E1 cells were stimulated with BMP9 (50 ng/ml) with or without MG132 (10μg/ml) for the indicated time. Total RNAs were isolated, reverse transcribed and analyzed by real-time polymerase chain reaction analyses. Relative mRNA expression levels of the indicated genes were calculated based on the Rpl13a mRNA level. Error bars represent SD. Statistical significance was determined by Student's t-test (* $P < 0.01$).

Figure 2.

Identification of responsible signaling pathways for BMP9-induced Hes1 expression in osteoblasts. (A) MC3T3-E1 cells were serum-starved for 4h, and preincubated with 1μM LDN193189 for 30 min. The cells were then stimulated with 50ng/ml BMP9 for the indicated time. Western blotting analysis was performed with the indicated antibodies. (B) MC3T3-E1 cells were serum-starved for 4h, and stimulated with 50ng/ml BMP9 for the indicated time with or without 30 min pretreatment by 1μM LY3039478, a gamma-secretase inhibitor. Western blotting analysis was performed with the indicated antibodies. (C) MC3T3-E1 cells were stimulated with 10ng/ml BMP9 for 1 hour with or without 30 min pretreatment by 1μM LY3039478. Total RNAs were isolated, reverse transcribed and analyzed by real-time PCR

analyses. Relative mRNA expression levels of the indicated genes were calculated based on the Rpl13a mRNA level. Fold induction of mRNA in comparison with the mRNA level of the unstimulated cells was shown. Error bars represent SD. (D) MC3T3-E1 cells were serum-starved for 4h, and preincubated with the indicated MAP kinase signal inhibitor (10μM U0126, 10μM SB203580, or 10μM SP600125) for 30 min. The cells were then stimulated with 50ng/ml BMP9 for the indicated time. (E) MC3T3-E1 TetOn pTre2-Hyg-mSmad7 cells were treated with or without 5ug/ml doxycycline for 24h, followed by stimulation with 50ng/ml BMP9 for the indicated time. Western blotting analysis was performed with the indicated antibodies. (F) MC3T3-E1 TetOn pTre2-Hyg-mSmad7 cells were treated as in (E). Total RNAs were isolated, reverse transcribed and analyzed by real-time PCR analyses. Relative mRNA expression levels of the indicated genes were calculated based on the Rpl13a mRNA level. Fold induction of mRNA in comparison with the mRNA level of the unstimulated cells was shown. Error bars represent SD. Statistical significance was determined by Student's t-test (* $P < 0.01$). (G) Small interference RNA (siRNA) designed for either Smad6 or Smad7 was introduced into MC3T3-E1 by using ScreenFect A plus. Total RNA was collected at 48 hours after siRNA introduction for real-time PCR analysis. Relative mRNA expression levels of the indicated genes were normalized by Rpl13a mRNA level. Fold changes in comparison with unstimulated-control siRNA transfected cells were shown. Statistical significance was assessed by one-way analysis of variance (ANOVA). ($P > 0.05$; * $P \leq 0.05$; ** $P \leq 0.01$; *** $P \leq 0.001$; **** $P \leq 0.0001$.) (H) MC3T3-E1 cells were transfected with Control, Smad6, or Smad7 siRNA followed by stimulation with 25 ng/ml BMP9 for the indicated times. Whole cell lysates were isolated and separated by SDS-PAGE. Target proteins were detected by Western blotting. (I) MC3T3-E1 cells were stimulated with 10 ng/ml BMP9 for 1 hour with or without 4-hour pretreatment by 1μM DMH1. Whole cell lysates were isolated and separated by SDS-PAGE. Target proteins were detected by Western blotting.

Figure 3.

Induction of Hes1 promoter activity by BMP9 in MC3T3-E1 cells. (A) Schematic diagram of the Hes1 promoter reporter constructs. Four pGL4.17 reporter plasmids containing variable lengths of mouse Hes1 gene 5'-upstream region are shown (pGL4-500, pGL4-1000, pGL4-1500, and pGL4-2000). (B) The Hes1-luciferase reporter plasmids were transiently transfected into MC3T3-E1 cells. At 48h after the transfection, cells were serum-starved for 16h and stimulated with 50ng/ml BMP9 for 6h. Luciferase activity in the cell lysates was analyzed with One Glo luciferase system. Error bars represent SD. The assay of each sample was done in triplicate and the average of three independent

experiments is shown.

Figure 4.

Identification of the transcription regulatory region of the mouse Hes1 gene. (A, B) The upstream nucleotide sequence of the transcriptional starting point in the mouse Hes1 gene. Five putative Smad binding sites were mutated by site-directed mutagenesis (Mut.A: -1346 to -1341, Mut.B: -1160 to -1155, Mut.C: -1139 to -1134, Mut.D: -1135 to -1130, Mut.E: -1036 to -1031) in the pGL4.17-1500 wild-type Hes1 promoter construct to analyze their functional significance. The mutated bases are shown in italic lower cases. (C) The mutated (Mut.A, Mut.B, Mut.C, Mut.D, Mut.E, and Mut.A&E) and the wild-type control constructs were transiently transfected into MC3T3-E1 cells. Luciferase reporter assay was performed as in Fig 3B. (D) After serum-starvation for 4h, MC3T3-E1 cells were stimulated with BMP9 (50ng/ml) for 1 hour. Chromatins were extracted and immunoprecipitated with an antibody against Smad1/5. qPCR analyses of the immunoprecipitated DNA were carried out. The positions of the PCR primer pairs are shown in (B).

Figure 5.

Functional roles of Hes1 on BMP9-induced osteoblast differentiation. (A) Small interference RNA (siRNA) designed for Hes1 was introduced into MC3T3-E1 by using ScreenFect A plus. At 48h after the transfection, MC3T3-E1 cells were stimulated with 10ng/ml BMP9 for the indicated time. Total RNAs were isolated, reverse transcribed and analyzed by real-time PCR analyses. Relative mRNA expression levels of the indicated genes were calculated based on the Rpl13a mRNA level. Fold changes in comparison with unstimulated-control siRNA transfected cells were shown. Error bars represent SD. Statistical significance was determined by Student's t-test (* $P < 0.01$).

Bone morphogenetic protein 9 (BMP9) directly induces Notch effector molecule Hes1 through the SMAD signaling pathway in osteoblasts

FIGURE LEGENDS

A

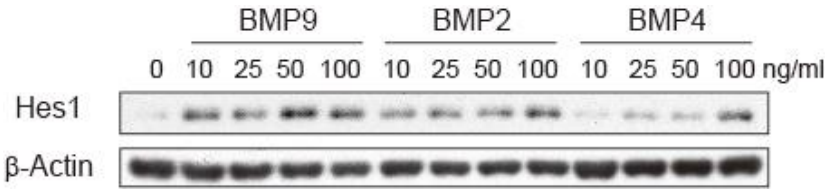

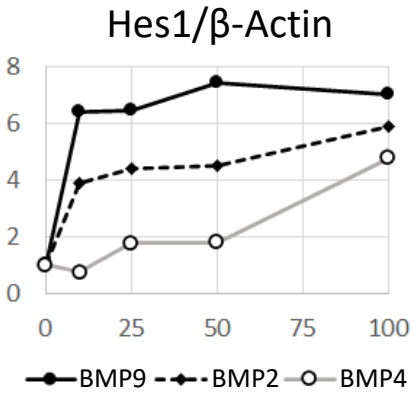

B

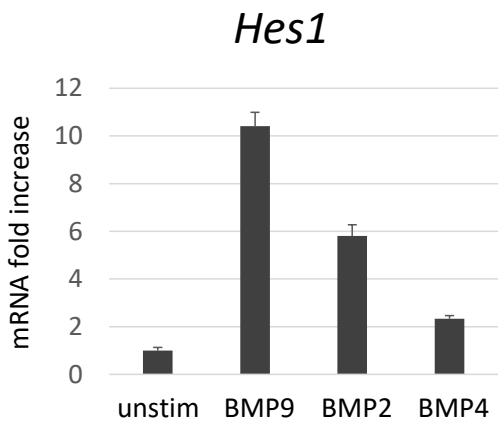

C

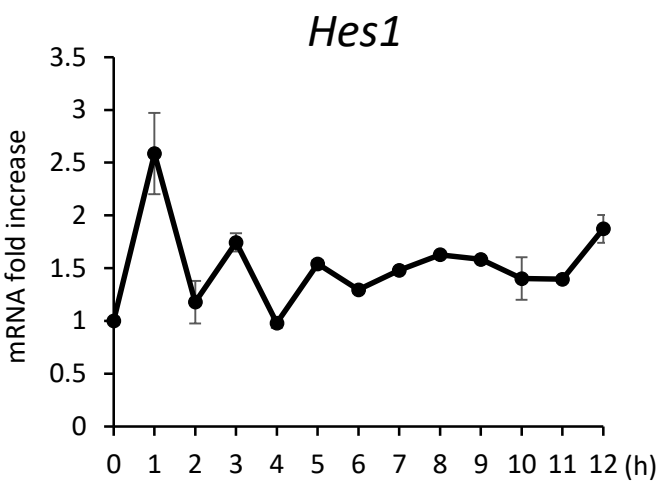

D

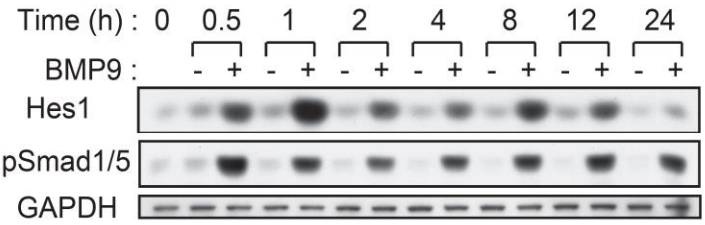

F

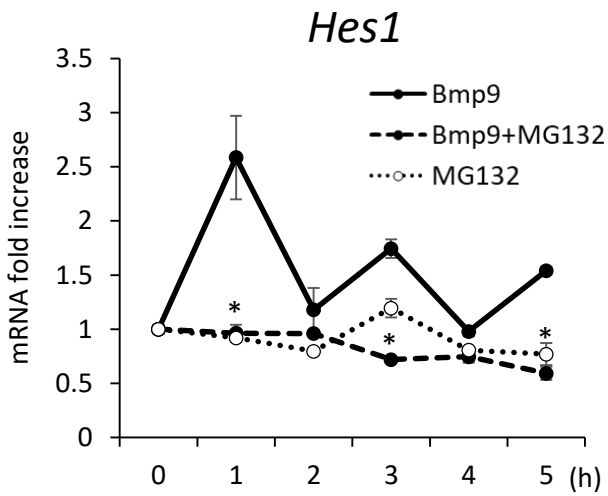

E

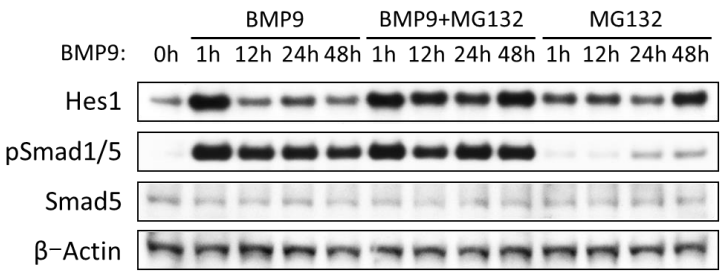

Figure 1. Hes1, a Notch effector molecule, is immediately induced by BMP9. (A) Dose response of Hes1 protein expression in BMP-stimulated osteoblasts. Calvaria-derived mouse primary osteoblasts were stimulated with indicated concentrations of BMP9, BMP2, or BMP4 for 1h. Cell lysates (10μg total protein for each lane) were analyzed with the indicated antibodies by western blotting. Photographical analyses of Hes1/β-Actin expression ratios are shown in the right graph. (B) After serum-starvation for 4h, mouse primary osteoblasts were stimulated with BMP9, BMP2, or BMP4 (10 ng/ml) for 1 hour. Total RNA was isolated and quantitative real-time PCR analyses were performed in triplicate using the specific primers for Hes1. Rpl13a was used as the endogenous control for normalization. (C) After serum-starvation for 4h, MC3T3-E1 cells were stimulated with BMP9 (50 ng/ml) for the indicated hours. Total RNA was isolated and reverse-transcribed. Quantitative real-time PCR analyses were performed in triplicate using the specific primers for Hes1. Rpl13a was used as the endogenous control for normalization. (D) After serum-starvation for 4h, MC3T3-E1 cells were stimulated with BMP9 (50 ng/ml) for the indicated hours. Cell lysates were analyzed with the indicated antibodies by Western blotting. (E) MC3T3-E1 cells were stimulated with BMP9 (10 ng/ml) with or without 10μg/ml of MG132 (Proteasome inhibitor) for the indicated time. Cell lysates were analyzed with the indicated antibodies by western blotting. (F) MC3T3-E1 cells were stimulated with BMP9 (50 ng/ml) with or without MG132 (10 μg/ml) for the indicated time. Total RNAs were isolated, reverse transcribed and analyzed by real-time polymerase chain reaction analyses. Relative mRNA expression levels of the indicated genes were calculated based on the Rpl13a mRNA level. Error bars represent SD. Statistical significance was determined by Student's t-test (* $P < 0.01$).

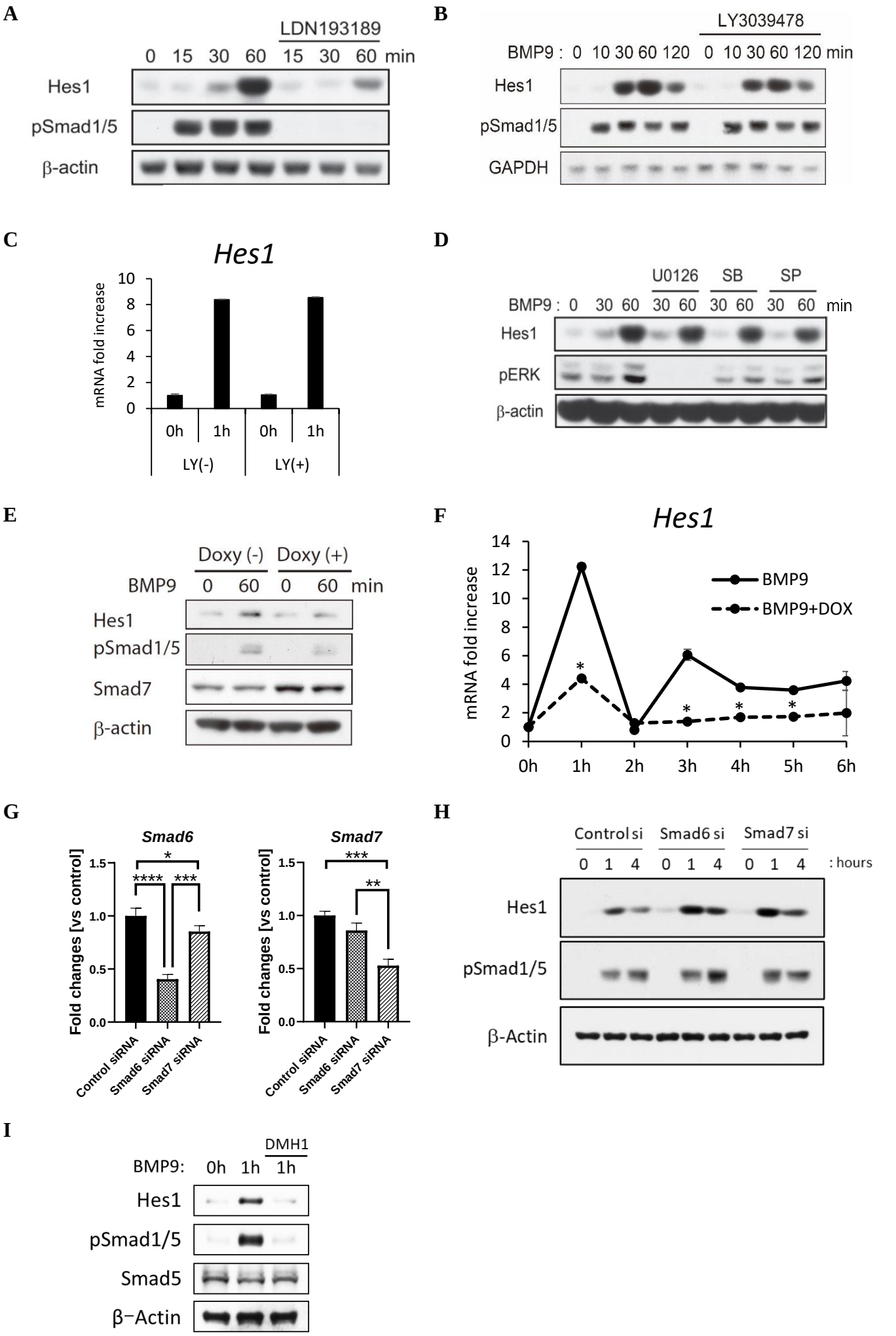
A
LDN193189
0 15 30 60 15 30 60 min
Hes1
pSmad1/5
β-actin
B
LY3039478
BMP9 : 0 10 30 60 120 0 10 30 60 120 min
Hes1
pSmad1/5
GAPDH
C
Hes1
mRNA fold increase
10
8
6
4
2
0
0h 1h 0h 1h
LY(-) LY(+)
D
U0126 SB SP
BMP9 : 0 30 60 30 60 30 60 30 60 min
Hes1
pERK
β-actin
E
Doxy (-) Doxy (+)
BMP9 0 60 0 60 min
Hes1
pSmad1/5
Smad7
β-actin
F
Hes1
mRNA fold increase
BMP9
BMP9+DOX
14
12
10
8
6
4
2
0
0h 1h 2h 3h 4h 5h 6h
G
Smad6
Smad7
Fold changes [vs control]
1.5
1.0
0.5
0.0
*
****
***
**
Control siRNA
Smad6 siRNA
Smad7 siRNA
H
Control si Smad6 si Smad7 si
0 1 4 0 1 4 0 1 4 : hours
Hes1
pSmad1/5
β-Actin
I
DMH1
BMP9: 0h 1h 1h
Hes1
pSmad1/5
Smad5
β−Actin

Figure 2. Identification of responsible signaling pathways for BMP9-induced Hes1 expression in osteoblasts. (A) MC3T3-E1 cells were serum-starved for 4h, and preincubated with 1μM LDN193189 for 30 min. The cells were then stimulated with 50 ng/ml BMP9 for the indicated time. Western blotting analysis was performed with the indicated antibodies. (B) MC3T3-E1 cells were serum-starved for 4h, and stimulated with 50 ng/ml BMP9 for the indicated time with or without 30 min pretreatment by 1μM LY3039478, a gamma-secretase inhibitor. Western blotting analysis was performed with the indicated antibodies. (C) MC3T3-E1 cells were stimulated with 10 ng/ml BMP9 for 1 hour with or without 30 min pretreatment by 1μM LY3039478. Total RNAs were isolated, reverse transcribed and analyzed by real-time PCR analyses. Relative mRNA expression levels of the indicated genes were calculated based on the Rpl13a mRNA level. Fold induction of mRNA in comparison with the mRNA level of the unstimulated cells was shown. Error bars represent SD. (D) MC3T3-E1 cells were serum-starved for 4h, and preincubated with the indicated MAP kinase signal inhibitor (10μM U0126, 10μM SB203580, or 10μM SP600125) for 30 min. The cells were then stimulated with 50 ng/ml BMP9 for the indicated time. (E) MC3T3-E1 TetOn pTre2-Hyg-mSmad7 cells were treated with or without 5 ug/ml doxycycline for 24h, followed by stimulation with 50 ng/ml BMP9 for the indicated time. Western blotting analysis was performed with the indicated antibodies. (F) MC3T3-E1 TetOn pTre2-Hyg-mSmad7 cells were treated as in (E). Total RNAs were isolated, reverse transcribed and analyzed by real-time PCR analyses. Relative mRNA expression levels of the indicated genes were calculated based on the Rpl13a mRNA level. Fold induction of mRNA in comparison with the mRNA level of the unstimulated cells was shown. Error bars represent SD. Statistical significance was determined by Student's t-test (* $P < 0.01$). (G) Small interference RNA (siRNA) designed for either Smad6 or Smad7 was introduced into MC3T3-E1 by using ScreenFect A plus. Total RNA was collected at 48 hours after siRNA introduction for real-time PCR analysis. Relative mRNA expression levels of the indicated genes were normalized by Rpl13a mRNA level. Fold changes in comparison with unstimulated-control siRNA transfected cells were shown. Statistical significance was assessed by one-way analysis of variance (ANOVA). ($P > 0.05$; * $P \leq 0.05$; ** $P \leq 0.01$; *** $P \leq 0.001$; **** $P \leq 0.0001$.) (H) MC3T3-E1 cells were transfected with Control, Smad6, or Smad7 siRNA followed by stimulation with 25 ng/ml BMP9 for the indicated times. Whole cell lysates were isolated and separated by SDS-PAGE. Target proteins were detected by Western blotting. (I) MC3T3-E1 cells were stimulated with 10 ng/ml BMP9 for 1 hour with or without 4-hour pretreatment by 1μM DMH1. Whole cell lysates were isolated and separated by SDS-PAGE. Target proteins were detected by Western blotting.

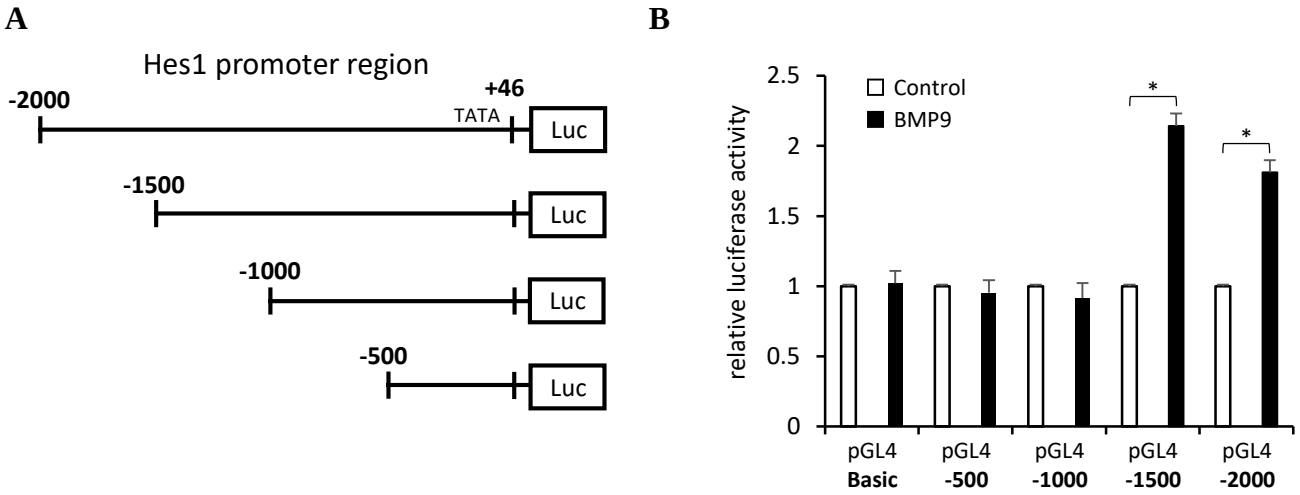

Figure 3. Induction of Hes1 promoter activity by BMP9 in MC3T3-E1 cells. (A) Schematic diagram of the *Hes1* promoter reporter constructs. Four pGL4.17 reporter plasmids containing variable lengths of mouse *Hes1* gene 5'-upstream region are shown (pGL4-500, pGL4-1000, pGL4-1500, and pGL4-2000). (B) The Hes1-luciferase reporter plasmids were transiently transfected into MC3T3-E1 cells. At 48h after the transfection, cells were serum-starved for 16h and stimulated with 50 ng/ml BMP9 for 6h. Luciferase activity in the cell lysates was analyzed with One Glo luciferase system. Error bars represent SD. The assay of each sample was done in triplicate and the average of three independent experiments is shown.

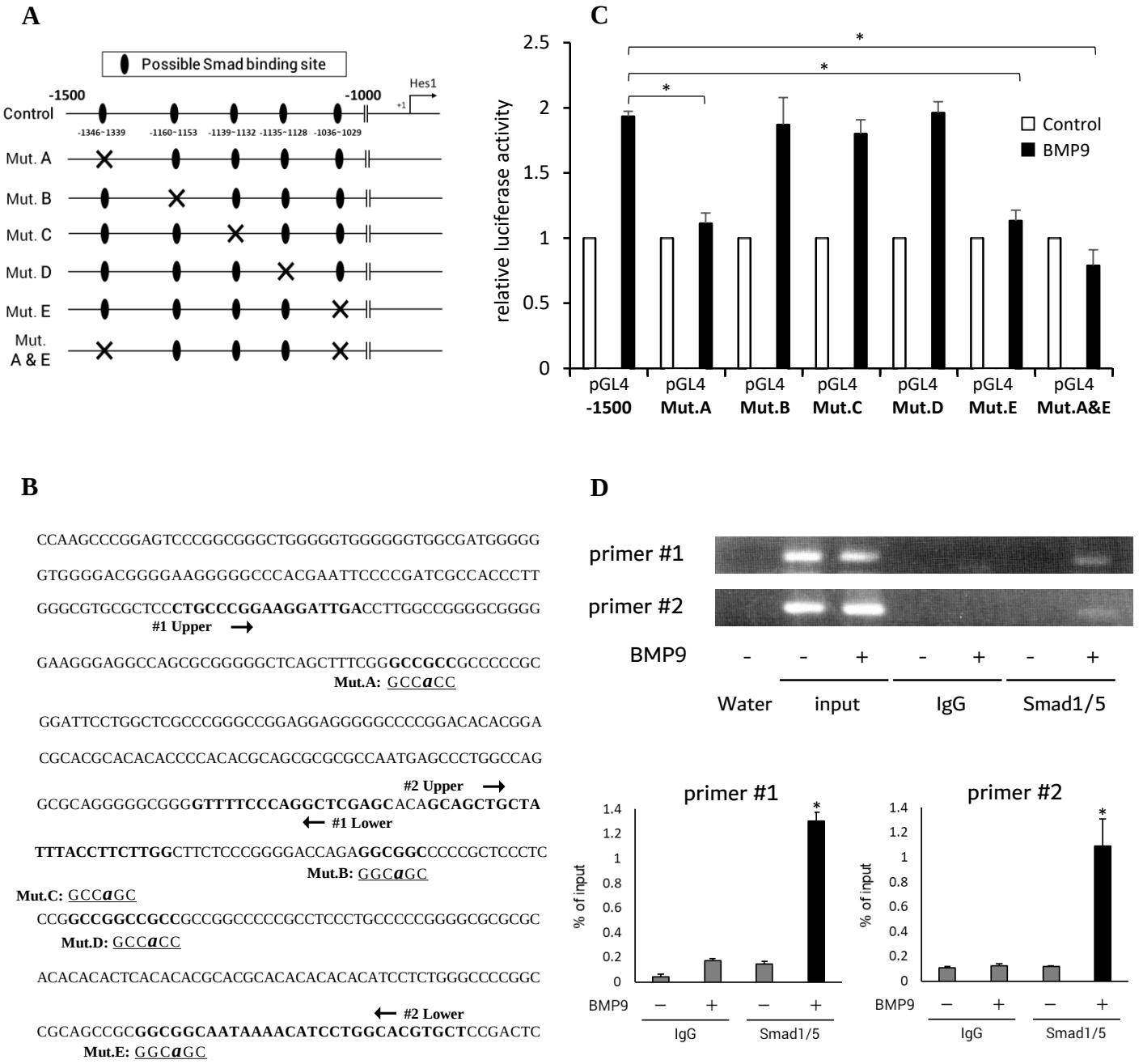

Figure 4. Identification of the transcription regulatory region of the mouse *Hes1* gene. (A,B) The upstream nucleotide sequence of the transcriptional starting point in the mouse *Hes1* gene. Five putative Smad binding sites were mutated by site-directed mutagenesis (Mut.A: -1346 to -1341, Mut.B: -1160 to -1155, Mut.C: -1139 to -1134, Mut.D: -1135 to -1130, Mut.E: -1036 to -1031) in the pGL4.17-1500 wild-type *Hes1* promoter construct to analyze their functional significance. The mutated bases are shown in italic lower cases. (C) The mutated (Mut.A, Mut.B, Mut.C, Mut.D, Mut.E, and Mut.A&E) and the wild-type control constructs were transiently transfected into MC3T3-E1 cells. Luciferase reporter assay was performed as in Fig 3B. (D) After serum-starvation for 4h, MC3T3-E1 cells were stimulated with BMP9 (50 ng/ml) for 1 hour. Chromatins were extracted and immunoprecipitated with an antibody against Smad1/5. qPCR analyses of the immunoprecipitated DNA were carried out. The positions of the PCR primer pairs are shown in (B).

A

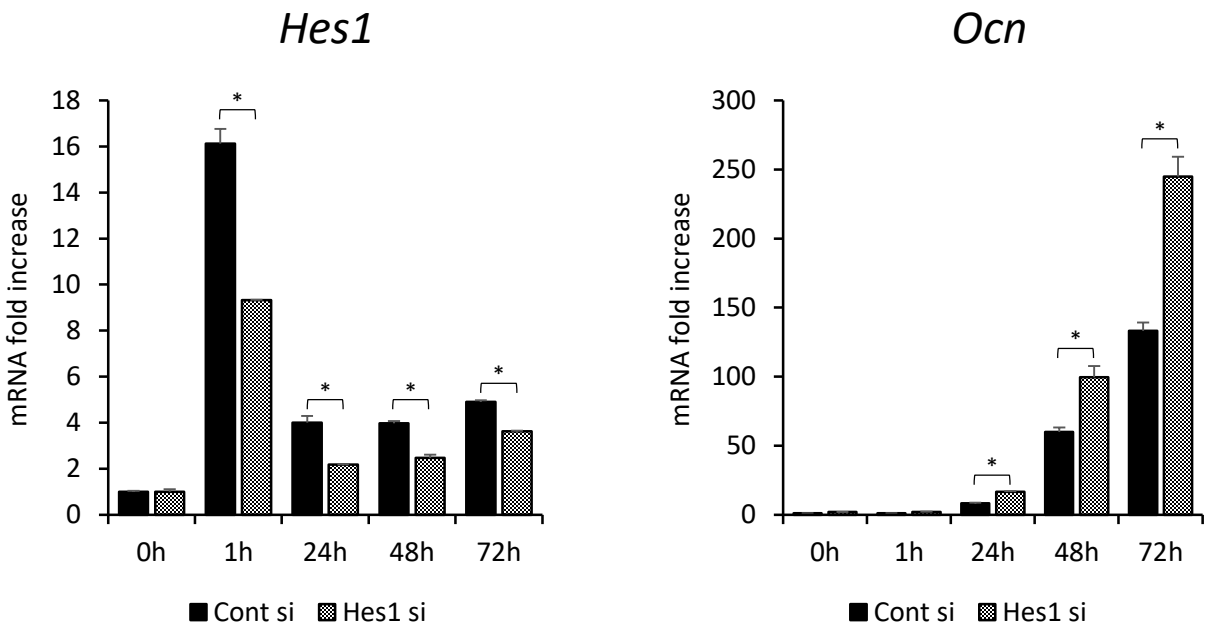

Figure 5. Functional roles of Hes1 on BMP9-induced osteoblast differentiation. (A) Small interference RNA (siRNA) designed for Hes1 was introduced into MC3T3-E1 by using ScreenFect A plus. At 48h after the transfection, MC3T3-E1 cells were stimulated with 10ng/ml BMP9 for the indicated time. Total RNAs were isolated, reverse transcribed and analyzed by real-time PCR analyses. Relative mRNA expression levels of the indicated genes were calculated based on the Rpl13a mRNA level. Fold changes in comparison with unstimulated-control siRNA transfected cells were shown. Error bars represent SD. Statistical significance was determined by Student's t-test (* $P < 0.01$).